

Electromagnetic corrections to the dominant two-pion exchange nucleon-nucleon potential

N. Kaiser

Physik Department T39, Technische Universität München, D-85747 Garching, Germany

Abstract

We calculate at two-loop order in chiral perturbation theory the electromagnetic corrections to the dominant two-pion exchange nucleon-nucleon interaction that is generated by the isoscalar πN contact-vertex proportional to the large low-energy constant c_3 . We find that the respective $2\pi\gamma$ -exchange potential contains sizeable isospin-breaking components which amount to about -1% of the strongly attractive isoscalar central 2π -exchange potential. The typical value of these novel charge-independence and charge-symmetry breaking central potentials is 0.3 MeV at a nucleon distance of $r = m_\pi^{-1} = 1.4\text{ fm}$. Our analytical result for this presumably dominant $2\pi\gamma$ -exchange interaction is in a form such that it can be easily implemented into phase-shift analyses and few-body calculations.

PACS: 12.20.Ds, 13.40.Ks, 21.30.Cb.

Isospin-violation in the nuclear force is a subject of current interest. Significant advances in the understanding of nuclear isospin-violation have been made in the past years by employing methods of effective field theory (in particular chiral perturbation theory). Van Kolck et al. [1] were the first to calculate (in a manifestly gauge-invariant way) the complete leading-order pion-photon exchange nucleon-nucleon interaction. In addition, the charge-independence and charge-symmetry breaking effects arising from the pion mass difference $m_{\pi^+} - m_{\pi^0} = 4.59\text{ MeV}$ and the nucleon mass difference $M_n - M_p = 1.29\text{ MeV}$ on the (leading order) two-pion exchange NN-potential have been worked out in Refs. [2, 3]. Recently, Epelbaum et al. [4] have continued this line of approach by deriving the subleading isospin-breaking 2π -exchange NN-potentials and classifying the relevant isospin-breaking four-nucleon contact terms. Moreover, some next-to-leading order corrections to the $\pi\gamma$ -exchange nucleon-nucleon potential (those proportional to the large isovector magnetic moment $\kappa_v = 4.7$ of the nucleon) as well as effects from virtual Δ -isobar excitation on the $\pi\gamma$ -exchange interaction have been calculated recently in Ref. [5].

The long-range (pion-induced) isospin-breaking potentials found so far turned out to be rather weak. Typically, their values at a distance of $r = m_\pi^{-1} = 1.4\text{ fm}$ lie below 50 keV in magnitude (see e.g. Tables I and II in Ref. [5]). More pronounced and therefore numerically significant are the isospin-breaking effects in the subleading 2π -exchange interaction (see herefore Figs. 8 and 10 in Ref. [4]). As in the isospin-conserving case this feature can be traced back to the large magnitude of the low-energy constants c_2 , c_3 and c_4 which enter as parameters in the second-order chiral pion-nucleon Lagrangian $\mathcal{L}_{\pi N}^{(2)}$. According to the numerical investigations made in Ref. [1], the inclusion of the (leading order) $\pi\gamma$ -exchange potential had negligible effects on the 1S_0 low-energy parameters and it led to only a tiny improvement in the fits of the NN-scattering data. With the partial cancellations through the next-to-leading order corrections [5] taken into account one may then conclude that the long-range $\pi\gamma$ -exchange interaction is too weak to explain the isospin-breaking NN-observables. One reason for this feature lies in the relative weakness of the 1π -exchange interaction itself. For example, its dominant (isovector) tensor potential amounts to only 9.2 MeV at a distance of $r = m_\pi^{-1} = 1.4\text{ fm}$. In comparison

to this the isoscalar central NN-attraction generated by chiral two-pion exchange comes out significantly larger (see e.g. Fig. 8 in Ref. [6]). Therefore one may expect that electromagnetic corrections to this strongest long-range NN-interaction, i.e. the chiral $2\pi\gamma$ -exchange interaction, will give rise to more substantial isospin-breaking effects. It is the purpose of the present short paper to evaluate a selected class of (presumably dominant) two-loop $2\pi\gamma$ -exchange diagrams. Now, since the isoscalar central NN-attraction comes mainly from the $\pi\pi NN$ contact-vertex proportional to the large low-energy constant c_3 , one naturally chooses for a first exploratory study the class of two-loop $2\pi\gamma$ -exchange diagrams with exactly one such c_3 -vertex. The essential long-distance information about the two-loop diagrams is contained in their spectral function, which we will evaluate here analytically.

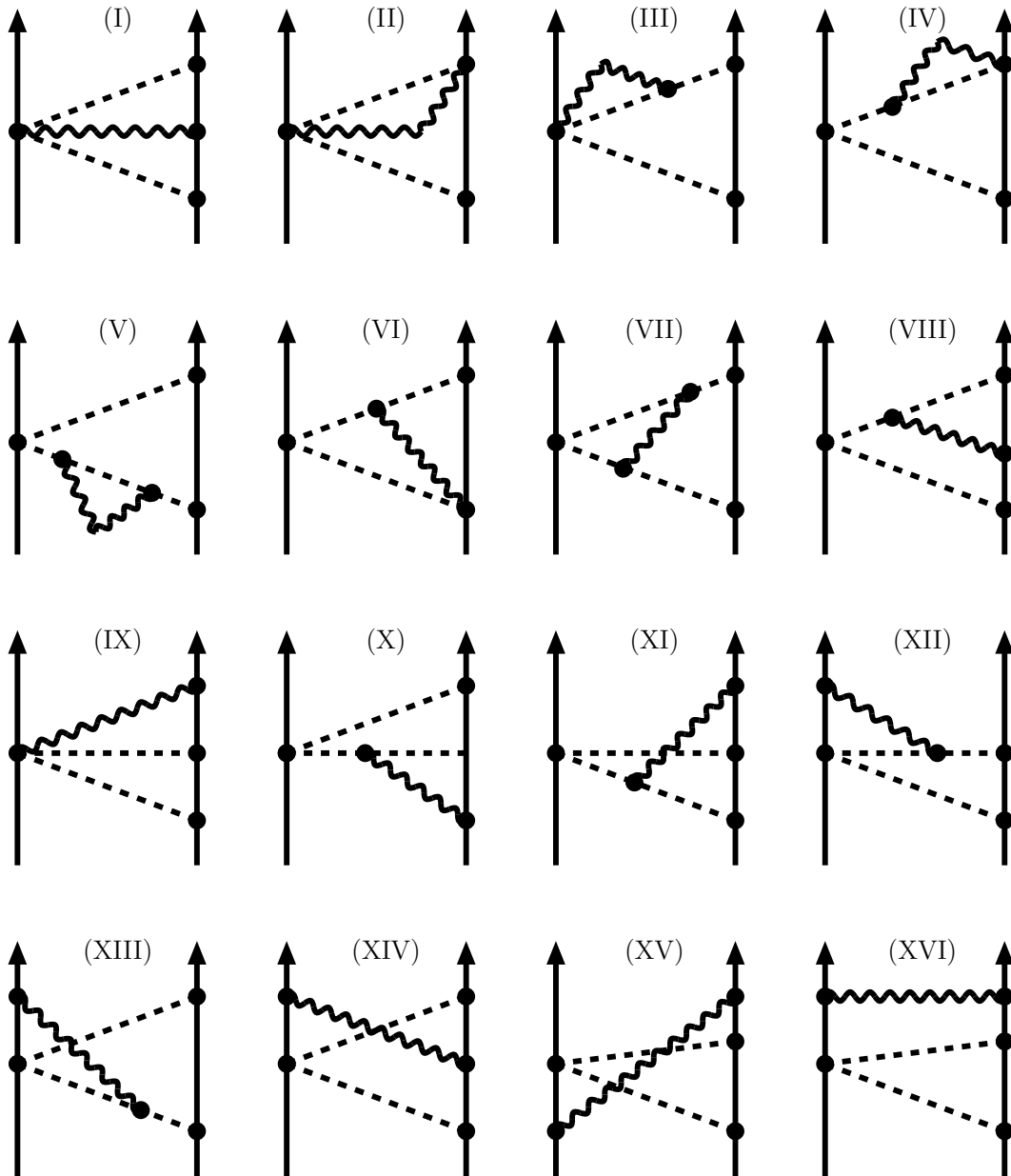


Fig. 1: Electromagnetic corrections to the dominant isoscalar central 2π -exchange NN-interaction generated by the $\pi\pi NN$ contact-vertex $-2ic_3f_\pi^{-2}\delta^{ab}q_a\cdot q_b$. Diagrams with the contact-vertex at the right nucleon line and diagrams turned upside-down are not shown. The spectral function $ImT(i\mu)$ is calculated by cutting the intermediate $\pi\pi\gamma$ three-particle state.

As a result, we do indeed find sizeable charge-independence and charge-symmetry breaking central potentials of magnitude 0.3 MeV at $r = m_\pi^{-1} = 1.4$ fm (for $c_3 = -3.3 \text{ GeV}^{-1}$). These seem to be the largest long-range isospin-breaking NN-potentials obtained so far. In order to test their phenomenological relevance they should be implemented into future phase-shift analyses and few-body calculations. As a result, we do indeed find sizeable charge-independence and charge-symmetry breaking central potentials of magnitude 0.3 MeV at $r = m_\pi^{-1} = 1.4$ fm (for $c_3 = -3.3 \text{ GeV}^{-1}$). These seem to be the largest long-range isospin-breaking NN-potentials obtained so far. In order to test their phenomenological relevance they should be implemented into future phase-shift analyses and few-body calculations.

Let us start with recalling the chiral 2π -exchange NN-interaction. Its dominant contribution to the isoscalar central channel comes from a triangle diagram involving one $\pi\pi NN$ contact-vertex with momentum-dependent coupling: $-2ic_3 f_\pi^{-2} \delta^{ab} q_a \cdot q_b$. The corresponding potential in coordinate space (obtained by a Laplace transformation) reads [6]:

$$\tilde{V}_C^{(2\pi)}(r) = \frac{3c_3 g_A^2}{32\pi^2 f_\pi^4} \frac{e^{-2z}}{r^6} (6 + 12z + 10z^2 + 4z^3 + z^4), \quad (1)$$

where $z = m_\pi r$. The occurring parameters are: $g_A = 1.3$ (the nucleon axial-vector coupling constant), $f_\pi = 92.4 \text{ MeV}$ (the pion decay constant), $m_\pi = 139.57 \text{ MeV}$ (the charged pion mass) and the low-energy constant $c_3 = -3.3 \text{ GeV}^{-1}$. The latter value is the average of $c_3 = -3.2 \text{ GeV}^{-1}$ and $c_3 = -3.4 \text{ GeV}^{-1}$ obtained by Entem et al. [7] and Epelbaum et al. [8, 9], respectively, in fits to NN-scattering phase shifts at next-to-next-to-next-to-leading order in the chiral expansion. The numerical values in the first row of Table I display the magnitude and r -dependence of this dominant isoscalar central 2π -exchange potential $\tilde{V}_C^{(2\pi)}(r)$.

Now we will add to the 2π -exchange triangle diagram a photon line which runs from one side to the other. There are five positions for the photon to start on the left hand side and seven positions to arrive at the right hand side. Leaving out those four diagrams which vanish in Feynman gauge (with photon propagator proportional to $g_{\mu\nu}$) we get the 16 representative diagrams shown in Fig. 1. Except for diagram (I) these are to be understood as being duplicated by horizontally reflected partners. A further doubling of the number of diagrams comes from interchanging the role of both nucleons.

We are interested here in the coordinate-space potentials generated by the $2\pi\gamma$ -exchange diagrams shown in Fig. 1. For that purpose it is sufficient to know their spectral function or imaginary part $\text{Im} T(i\mu)$. Making use of (perturbative) unitarity in the form of the Cutkosky cutting rule we can calculate the two-loop spectral functions as integrals of the (subthreshold) $\bar{N}N \rightarrow \pi\pi\gamma \rightarrow \bar{N}N$ transition amplitudes over the Lorentz-invariant $2\pi\gamma$ three-particle phase space [10]. In the (conveniently chosen) center-of-mass frame this leads to two angular integrations and two integrals over the pion energies. Due to the heavy nucleon limit ($M_N \rightarrow \infty$) and the masslessness of the photon ($m_\gamma = 0$) several simplifications occur and therefore most of these integrations can actually be performed in closed analytical form. For a concise presentation of our results it is also advantageous to scale out all common (dimensionful) parameters from the spectral function:

$$\text{Im} T(i\mu) = \frac{\alpha c_3 g_A^2 m_\pi^3}{\pi (4f_\pi)^4} S\left(\frac{\mu}{m_\pi}\right), \quad (2)$$

and to work with the dimensionless variable $u = \mu/m_\pi$, where $\mu \geq 2m_\pi$ denotes the $\pi\pi\gamma$ -invariant mass and $\alpha = 1/137.036$ is the fine-structure constant. Without going into further technical details, we enumerate now the contributions of the 16 representative $2\pi\gamma$ -exchange

diagrams shown in Fig. 1 to the dimensionless spectral function $S(u)$. We find for $u \geq 2$:

$$S(u)^{(I)} = (2 - \tau_1^3 - \tau_2^3) \left\{ \frac{u^3}{2} - 5u + 4 + \frac{2}{u-1} + \frac{2}{u} \ln(u-1) \right\}, \quad (3)$$

where $\tau_{1,2}^3$ denotes the third components of the usual isospin operators.

$$S(u)^{(II)} = 36u - 2u^3 - 48 - \frac{8}{u-1} - \frac{40}{u} \ln(u-1), \quad (4)$$

$$S(u)^{(III)} = 9u^3 - 12u^2 - 54u + 84 + \frac{4}{u}(14u^2 - 11 - 3u^4) \ln(u-1), \quad (5)$$

$$S(u)^{(IV)} = 7u^3 - 12u^2 - 26u + 44 + \frac{4}{u}(8u^2 - 5 - 3u^4) \ln(u-1), \quad (6)$$

$$S(u)^{(V)} = 16u^2 - 12u^3 + 56u - 80 - \frac{16}{u}(u^2 - 1)^2 \ln(u-1) \quad (7)$$

$$S(u)^{(VI)} = 3u^3 - 8u^2 - 22u + 48 + \frac{4}{u-1} + \frac{44}{u} \ln(u-1) + \frac{16}{u}(u^2 - 2) \int_1^{u/2} \frac{dx}{y} \ln \frac{u(x+y) - 1}{u(x-y) - 1}, \quad (8)$$

with the abbreviation $y = \sqrt{x^2 - 1}$.

$$\begin{aligned} S(u)^{(VII)} &= 20u^2 - 9u^3 + 22u - 52 + \frac{4}{u}(5u^4 - 16u^2 + 11) \ln(u-1) \\ &+ \frac{8}{u^2}(u^2 - 2) \int_1^{u/2} dx \frac{(ux - 1)(4 - u^2 - 2ux)}{(u - 2x)y} \ln \frac{u(x+y) - 1}{u(x-y) - 1}, \end{aligned} \quad (9)$$

$$\begin{aligned} S(u)^{(VIII)} &= (2 - \tau_1^3 - \tau_2^3) \left\{ 3u^2 + 6u - 11 + \left(u^3 - 2u - \frac{2}{u} \right) \ln(u-1) \right. \\ &\left. - \frac{3u^3}{2} - \frac{1}{u-1} + \frac{2}{u}(u^2 - 2) \int_1^{u/2} dx \frac{ux - 1}{y} \ln \frac{u(x+y) - 1}{u(x-y) - 1} \right\}, \end{aligned} \quad (10)$$

$$\begin{aligned} S(u)^{(IX)} &= (2 + \tau_1^3 + \tau_2^3) \left\{ \frac{u^3}{2} - 5u + 4 + \frac{2}{u-1} + \frac{2}{u} \ln(u-1) \right. \\ &\left. + \frac{1}{3}(26 - 5u^2)\sqrt{u^2 - 4} - \frac{8}{u} \ln \frac{u + \sqrt{u^2 - 4}}{2} \right\}, \end{aligned} \quad (11)$$

$$\begin{aligned} S(u)^{(X)} &= (2 + \tau_1^3 + \tau_2^3) \left\{ u^2 - \frac{u^3}{4} + \frac{3u}{2} - 5 + \left(u^3 - 4u + \frac{3}{u} \right) \ln(u-1) \right. \\ &+ \frac{8}{3}(1 - u^2)\sqrt{u^2 - 4} + \left(4u^3 - 10u + \frac{8}{u} \right) \ln \frac{u + \sqrt{u^2 - 4}}{2} \\ &\left. + \frac{4}{u}(u^2 - 2) \int_1^{u/2} \frac{dx}{u - 2x} \left[uy + (1 - u^2) \ln \frac{u - x + y}{u - x - y} \right] \right\}, \end{aligned} \quad (12)$$

$$\begin{aligned} S(u)^{(XI)} &= S(u)^{(X)} + (2 + \tau_1^3 + \tau_2^3) \left\{ u^2 - u^3 + \left(6u - u^3 - \frac{8}{u} \right) \ln(u-1) \right. \\ &\left. + 3u - 1 - \frac{1}{u-1} + \frac{2}{u}(u^2 - 2) \int_1^{u/2} dx \frac{ux - 1}{y} \ln \frac{u(x+y) - 1}{u(x-y) - 1} \right\}, \end{aligned} \quad (13)$$

$$\begin{aligned}
S(u)^{\text{(XII)}} &= (\tau_1^3 + \tau_2^3 + 2\tau_1^3\tau_2^3) \left\{ \frac{u^3}{4} - u^2 - \frac{3u}{2} + 5 + \left(4u - u^3 - \frac{3}{u}\right) \ln(u-1) \right. \\
&\quad - 3u^2\sqrt{u^2-4} + \left(4u^3 - 6u + \frac{8}{u}\right) \ln \frac{u + \sqrt{u^2-4}}{2} \\
&\quad \left. + \frac{4}{u}(u^2-2) \oint_1^{u/2} \frac{dx}{u-2x} \left[uy + (1-u^2) \ln \frac{u-x+y}{u-x-y} \right] \right\}, \quad (14)
\end{aligned}$$

$$S(u)^{\text{(XIII)}} = S(u)^{\text{(XII)}} + (\tau_1^3 + \tau_2^3 + 2\tau_1^3\tau_2^3) \left\{ 2u^2 - \frac{u^3}{2} + 3u - 10 + \left(2u^3 - 8u + \frac{6}{u}\right) \ln(u-1) \right\}, \quad (15)$$

$$S(u)^{\text{(XIV)}} = (3 + \tau_1^3 + \tau_2^3 - \tau_1^3\tau_2^3) \left\{ \left(\frac{u^2}{2} - 3\right) \sqrt{u^2-4} + \frac{4}{u} \ln \frac{u + \sqrt{u^2-4}}{2} \right\}, \quad (16)$$

$$S(u)^{\text{(XV)}} + S(u)^{\text{(XVI)}} = 0. \quad (17)$$

The exact cancellation between diagram (XV) and the irreducible part of diagram (XVI) has the same kinematical reason as the cancellation between the crossed box and (the irreducible part of the) planar box diagram, which has been discussed in detail in Ref. [6]. We have carefully checked gauge-invariance. The total (dimensionless) spectral function $S(u)$ stays ξ -independent when adding a longitudinal part to the photon propagator: $g_{\mu\nu} \rightarrow g_{\mu\nu} + \xi k_\mu k_\nu$. This property holds already separately in the subclasses of diagrams: (I)+(VIII), (II)+(IV)+(VI), (III)+(V)+(VII), (IX)+(X)+(XI), (XII)+(XIII) and (XIV). The "encircled" integrals appearing in Eqs.(9,12,14) involve the following regularization prescription:

$$\oint_1^{u/2} dx \frac{f(x)}{u-2x} = \int_1^{u/2} dx \frac{f(x) - f(u/2)}{u-2x}. \quad (18)$$

This regularization prescription eliminates from some diagrammatic contributions ((V), (VII), (X), (XI), (XII), (XIII)) to the spectral function an infrared singularity arising from the emission of soft photons ($\bar{N}N \rightarrow \pi\pi\gamma_{\text{soft}}$). In the $2\pi\gamma$ phase space (an oval-shaped region in the $\omega_1\omega_2$ -plane spanned by the pion energies) the singularity is located at that extremal boundary point ($\omega_{1,2} = \mu/2$) where the photon energy $\mu - \omega_1 - \omega_2$ becomes identical to zero. The singular factor $(u-2x)^{-1}$ in Eq.(18) stems from a pion propagator. The regularization prescription defined in Eq.(18) is equivalent to the familiar "plus"-prescription [11] employed commonly for parton splitting functions in order to eliminate there an analogous infrared singularity due to soft gluon radiation.¹ We note as an aside that the non-elementary integrals ($\int_1^{u/2} dx \dots$) in Eqs.(8–14) can be solved in terms of dilogarithms and squared logarithms of the argument $(u + \sqrt{u^2-4})/2$ [12].

Let us first discuss some generic properties. All contributions to the dimensionless spectral function $S(u)$ vanish at the $\pi\pi\gamma$ -threshold $u = 2$. This is markedly different from the original one-loop two-pion exchange triangle diagrams which possess the discontinuous spectral function $S(u)^{(2\pi)} = -12\pi(\alpha u)^{-1}(u^2-2)^2\theta(u-2)$ with a non-vanishing threshold value. The leading threshold behavior of the total dimensionless spectral function $S(u)$ is: $S(u) = 64(1 + \tau_1^3)(1 + \tau_2^3)(1 - \ln 2)\sqrt{u-2} + \mathcal{O}(u-2)$ and it comes exclusively from the four diagrams (X)–(XIII). Such a square-root like growth implies an asymptotic tail of the coordinate-space potential of the form $e^{-2m_\pi r} r^{-5/2}$ for $r \rightarrow \infty$, whereas at short distances $r \rightarrow 0$ the potential develops a $r^{-6} \ln^2(m_\pi r)$

¹It would of course be desirable to extend the present calculational framework (by including various radiation diagrams etc.) such that the overall infrared finiteness could be demonstrated in detail. This goes beyond the scope of the present work and therefore we stay with the physically well-founded regularization prescription Eq.(18).

singularity, somewhat stronger than that of $\tilde{V}_C^{(2\pi)}(r)$ written in Eq.(1). At any intermediate nucleon distance r the $2\pi\gamma$ -exchange central potential in coordinate-space $\tilde{V}_C^{(2\pi\gamma)}(r)$ can be calculated from the spectral function $\text{Im}T(i\mu)$ via a modified Laplace transformation:

$$\begin{aligned}\tilde{V}_C^{(2\pi\gamma)}(r) &= -\frac{1}{2\pi^2 r} \int_{2m_\pi}^{\infty} d\mu \mu e^{-\mu r} \text{Im}T(i\mu) \\ &= \tilde{V}_C^{(0)}(r) + \tau_1^3 \tau_2^3 \tilde{V}_C^{(\text{cib})}(r) + (\tau_1^3 + \tau_2^3) \tilde{V}_C^{(\text{csb})}(r),\end{aligned}\quad (19)$$

where we have given in the second line of Eq.(19) its decomposition into isospin-conserving (0), charge-independence breaking (cib), and charge-symmetry breaking (csb) parts. We note again as an aside that the (partial) contributions to the potential $\tilde{V}_C^{(2\pi\gamma)}(r)$ coming from the terms in Eqs.(3–16) without integrals can be represented by the exponential function e^{-2z} , the exponential-integral function $e^{-z}E_1(z)$, and two modified Bessel functions $K_{0,1}(2z)$, each multiplied by a pure polynomial in $1/z$ of degree 6 or lower, where $z = m_\pi r$ [12].

We are now in the position to present numerical results for the dominant $2\pi\gamma$ -exchange nucleon-nucleon potentials. The numbers in the second, third, and fourth row of Table I show the dropping of the central potentials $\tilde{V}_C^{(0)}(r)$, $\tilde{V}_C^{(\text{cib})}(r)$ and $\tilde{V}_C^{(\text{csb})}(r)$ with the nucleon distance r in the range $1.0 \text{ fm} \leq r \leq 2.1 \text{ fm}$. Note that all potentials are given in units of MeV. One observes that the repulsive charge-independence breaking (cib) potential and the repulsive charge-symmetry breaking (csb) potential are approximately equal and about half as strong as the isospin-conserving one. Their magnitudes (for example, 0.3 MeV at a distance of $r = 1.4 \text{ fm}$) are exceptionally large in comparison to all so far known isospin-breaking NN-potentials generated by long-range pion-exchange. The dominant contributions to $\tilde{V}_C^{(\text{cib})}(r)$ and $\tilde{V}_C^{(\text{csb})}(r)$ come from the four diagrams (X)–(XIII). This selective feature is consistent with the above-mentioned leading threshold behavior of the spectral function $S(u)$ and the associated large- r asymptotics.

r [fm]	1.0	1.1	1.2	1.3	1.4	1.5	1.6	1.7	1.8	1.9	2.0	2.1
$\tilde{V}_C^{(2\pi)}$	-221	-121	-69.3	-41.4	-25.6	-16.3	-10.6	-7.05	-4.78	-3.30	-2.31	-1.64
$\tilde{V}_C^{(0)}$	6.47	3.25	1.72	0.953	0.547	0.325	0.198	0.124	0.079	0.051	0.034	0.023
$\tilde{V}_C^{(\text{cib})}$	3.54	1.78	0.948	0.526	0.303	0.180	0.110	0.069	0.044	0.029	0.019	0.013
$\tilde{V}_C^{(\text{csb})}$	3.57	1.80	0.956	0.530	0.305	0.182	0.111	0.070	0.045	0.029	0.019	0.013

Table I: The dominant isoscalar central 2π -exchange NN-potential $\tilde{V}_C^{(2\pi)}(r)$, and electromagnetic corrections to it, as a function of the nucleon distance r . The values in the third and fourth row correspond to the isospin-violating potentials $\tilde{V}_C^{(\text{cib})}(r)$ and $\tilde{V}_C^{(\text{csb})}(r)$. All potentials are given in units of MeV.

It is also instructive to compare the isospin-violating $2\pi\gamma$ -exchange potentials with the isospin-conserving 2π -exchange potential $\tilde{V}_C^{(2\pi)}(r)$. Their relative ratio of about -1 percent is consistent with the usual rule of thumb estimate, namely $\alpha/\pi \simeq 1/430$ times a numerical factor. In the present case this numerical factor is not just 1 but of the order 5, due to the large number of contributing diagrams (in total there were 54 non-vanishing diagrams).

We have also computed the $2\pi\gamma$ -exchange central potentials proportional to the other large low-energy constant $c_2 = 3.3 \text{ GeV}^{-1}$. At a reference distance of $r_0 = 1.4 \text{ fm}$ one finds the values $\tilde{V}_C^{(0)}(r_0) = -8.54 \text{ keV}$, $\tilde{V}_C^{(\text{cib})}(r_0) = -23.4 \text{ keV}$ and $\tilde{V}_C^{(\text{csb})}(r_0) = -14.8 \text{ keV}$. These potentials are in fact more than an order of magnitude smaller than their counterparts generated by the c_3 -vertex. Furthermore, as expected the $2\pi\gamma$ -exchange central potentials arising from the c_1 -vertex are small. With $c_1 = -0.8 \text{ GeV}^{-1}$ we get $\tilde{V}_C^{(0)}(r_0) = 23.4 \text{ keV}$, $\tilde{V}_C^{(\text{cib})}(r_0) = 8.40 \text{ keV}$ and

$\tilde{V}_C^{(\text{csb})}(r_0) = 9.78 \text{ keV}$. This confirms our assumption made about the dominant $2\pi\gamma$ -exchange NN-potential.

In summary we have calculated in this work the electromagnetic corrections to the dominant two-pion exchange nucleon-nucleon interaction that is generated by the isoscalar πN contact-vertex proportional to the large low-energy constant $c_3 = -3.3 \text{ GeV}^{-1}$. We have evaluated analytically the spectral function of a large class of 70 two-loop $2\pi\gamma$ -exchange diagrams. The result for the total spectral function is manifestly gauge-invariant. An infrared singularity related to soft photon emission which occurs in some contributions has been regularized by a prescription analogous to the one employed commonly for parton splitting functions. As a major result we have found that the $2\pi\gamma$ -exchange potential contains sizeable isospin-breaking components which amount to about -1% of the strongly attractive isoscalar central 2π -exchange potential. A typical value of the charge-independence and charge-symmetry breaking central potential is 0.3 MeV at a nucleon distance of $r = m_\pi^{-1} = 1.4 \text{ fm}$. Our analytical result for this novel and exceptionally large isospin-violating long-range nuclear force has been presented in a form such that it can be easily implemented into phase-shift analyses and few-body calculations. For completeness one should also calculate the $2\pi\gamma$ -exchange diagrams proportional to the remaining large low-energy constant $c_4 \simeq 3.4 \text{ GeV}^{-1}$ which generate (isospin-violating) spin-spin and tensor potentials. Some of the technical advantages arising from the Lorentz-scalar nature of the c_3 -vertex are then, however, no more available. The issue of (overall) infrared finiteness should also be further explored. Work along this line is in progress.

References

- [1] U. van Kolck, M.C.M. Rentmeester, J.L. Friar, T. Goldman and J.J. de Swart, *Phys. Rev. Lett.* **80**, 4386 (1998).
- [2] J.L. Friar and U. van Kolck, *Phys. Rev.* **C60**, 034006 (1999).
- [3] J.L. Friar, U. van Kolck, G.L. Payne and S.A. Coon, *Phys. Rev.* **C68**, 024003 (2003).
- [4] E. Epelbaum and Ulf-G. Meißner, *Phys. Rev.* **C72**, 044001 (2005).
- [5] N. Kaiser, *Phys. Rev.* **C73**, 044001 (2006).
- [6] N. Kaiser, R. Brockmann and W. Weise, *Nucl. Phys.* **A625**, 758 (1998).
- [7] D.R. Entem and R. Machleidt, *Phys. Rev.* **C68**, 041001 (2003); and references therein.
- [8] E. Epelbaum, W. Glöckle, and Ulf-G. Meißner, *Nucl. Phys.* **A747**, 362 (2005); and references therein.
- [9] E. Epelbaum, *Prog. Part. Nucl. Phys.* (2006), in print; nucl-th/0509032.
- [10] N. Kaiser, *Phys. Rev.* **C62**, 024001 (2000).
- [11] M.E. Peskin and D.V. Schroeder, “Quantum Field Theory”, Addison-Wesley Publishing Company (1995); chapter 17.5.
- [12] These somewhat lengthy formulas can be obtained from the author upon request. The information given here in Eqs.(2-19) is already sufficient for an easy and accurate numerical evaluation of the potential $\tilde{V}_C^{(2\pi\gamma)}(r)$.